Stability Of Long Liquid Columns

WL-FPM-STACO

I. Martínez, J.M. Perales, J. Meseguer
Lamf-ETSIA, UPM, Madrid, Spain

Abstract

A description of this experiment, the data analysis performed and the results obtained are presented. Three successful runs were executed: the first one included a detailed oscillation test around a low eigenfrequency of the liquid column, the second was a stretching at constant volume until breakage, and the third one included an unexplained instability of an unequal-discs liquid column. The main diagnostic is the image analysis of the recorded videotape, and the most important result is that a residual axial acceleration of less than 5 μg is deduced from this SL-D-2 experiment, in contrast to the 70 μg deduced from the SL-D1 experiment in 1985.

Keywords: Capillarity, liquid bridge, microgravity, stability, g-jitter, floating zone, Spacelab

Introduction

A liquid bridge is a liquid mass spanning between two solid supports and held solely by capillary forces (surface tension and wetting constraint). It is established once in flight by feeding liquid from a syringe through a centre hole in one of the support discs (the lower one in Fig. 1), while separating the discs (the feeding one is moved) proportionally, to avoid spillage. The liquid used is a silicone-oil 10 times more viscous than water (5 times for the last run). The working length of the liquid column is 85 mm. The two solid supports are made of aluminum of 30 mm in diameter with a sharp cutback (30° edge) to prevent liquid spreading over the edges. This choice of geometry allows a direct comparison with other TEXUS experiments where discs of 30 mm in diameter separated 86 mm were used to hold a cylindrical liquid column (35 mm discs were used in SL-D1 and 40 mm discs on SL-1). Research on this topic at this institution started in 1974 as an answer to an ESA call for ideas for Spacelab experimentation [1-5]. The ESA-AFPM, a multi-user facility similar to the Fluid Physics Module (FPM) used in SL-1 and SL-D1, was used in SL-D-2. Diagnosis is based on the outer-shape analysis from image recording.

Scientific Objective

The aim of this experiment is to measure the outer shape deformation of long liquid bridges near their stability limit under microgravity, caused by g-jitter and by some controlled mechanical disturbances (change of geometry, change of volume, rotation and vibration). The liquid bridge configuration has, aside of its own relevance in fluid-mechanics and interface science, a well-known application in materials processing, particularly in the floating zone technique of crystal growth in the semiconductor industry. As a spin-off of this research, this configuration has proved to be a unique weak-force transducer at very low frequencies.

To better sense the small forces foreseen, the liquid column has to be as large as possible. Although the AFPM test chamber allows for up to 130 mm span between end plates, the conical perspective dictates that a maximum of some $L=90$ mm long column can be well accommodated in the bright field of view (by means of protruding discs). The correspond-

ing diameter for instability at that length is $D=L/\pi=28$ mm and, to be in the safe side, a nominal diameter of $D=30$ mm was chosen. A lot of stability diagrams for this geometry and different stimuli were computed to asses the effect of an axial acceleration, a centrifugal force field, a departure from the cylindrical volume, different disc sizes and column slenderness.

A known handicap of present-day experimentation in space is the lack of repetitions of trials due to the scarcity of microgravity flights and crew-time, and the uniqueness of Spacelab hardware, so that it was top priority of STACO to quickly verify the results of SL-D1, and because an equivalent Bond number $Bo=0.007$ was deduced from the SL-D1-FPM-FLIZ experiment and there was no reason to expect a different behaviour, the SL-D-2-FPM-STACO experiment foresaw the use of unequal discs of 30 mm and 28 mm in a second run to precisely counterbalance the expected deformation and better quantify this effect.

The particular goals of this SL-D-2 experiment [4] can then be grouped as follows:

- Sense background g-jitter and discern against the SL-D1 experiment results.
- Force oscillations very near a low eigenfrequency (the second one).
- Measure breaking lengths of a stretching equal-discs column.
- Measure breaking lengths of a stretching unequal-discs column.
- Measure breaking rotation rate of an isorotating column.

Uncertainty analysis is important to any experiment, but particularly crucial to STACO since we try to measure the effect on a 60 cm^3 liquid column of applied forces in the range 10^{-5} N to 10^{-7} N.

Experiment Description

The equipment used, the AFPM, is described elsewhere, but it seems appropriate here to look in detail to the uncertainties in the data analysis associated with the equipment, as well as with the working liquid.

The AFPM is a high-precision apparatus but, being a multi-user facility, its wide operating ranges have forced some tolerances that impact on the STACO experiment. For instance, a precision for an axial oscillation of 0.01 Hz from 0.1 Hz to 5 Hz is very good for a multiple-degrees-of-freedom mechanism, but it happens that the first eigenfrequency of the liquid bridge under study is just below 0.1 Hz, and a 0.01 Hz resolution for the second eigenfrequency at 0.4 Hz is not very much.

Most other AFPM tolerances were judged irrelevant for STACO. For instance, for disc separation L and volume injection V, the AFPM accuracies are $\Delta L_{min} = 0.1$ mm, $dL/dt_{min} = 0.04$ mm/s, $\Delta dL/dt = \pm 0.02$ mm/s and $\Delta V_{min} = 0.5$ cm^3, $dV/dt_{min} = \pm 0.5$ cm^3/s, $\Delta dV/dt = 0.05$ cm^3/s, so that for speed values for cylindrical injection set to $dL/dt = 0.72$ mm/s and $dV/dt = 0.50$ cm^3/s, they are digitally controlled to $dL/dt = 0.72 \pm 0.02$ mm/s and $dV/dt = 0.50 \pm 0.05$ cm^3/s (or worst, as in the first cylindrical injection, set to $dV/dt = 0.50$ cm^3/s and having a value of $dV/dt = 0.40 \pm 0.05$ cm^3/s deduced from the AFPM data).

However in some cases a more detailed analysis after flight cast some doubts on the irrelevance of AFPM tolerances, as for the three fixed-frequency trials in Run 1, that were intended to be equispaced near the second eigenfrequency (at 0.40 Hz, 0.41 Hz and 0.42 Hz), what seems inconsistent with the AFPM accuracy of $\Delta f_{min} = 0.01$ Hz (related AFPM accuracies are $df/dt_{min} = 1/90$ Hz/s and $\Delta a_{min} = 0.1$ mm).

A reservoir with 1 litre of Dow Corning silicone oil of viscosity $\nu = 10^{-6}$ m^2/s (10 cSt) was used for STACO and LICOR experiments. To be able to visualise the internal motion, the liquid was seeded with 0.2 gram/litre of tracers (Eccospheres from Emerson and Cummings, silver-coated in the ULB-MRC, with density of 960–1000 kg/m^3 and diameter of 100±20 μm). The nominal illumination however was such that the column edge visualisation was enhanced and the tracers were invisible.

Five working discs were flown for STACO, but only the three metallic ones were used, all of them protruding from the AFPM base-plate and with a sharp cutback at the working surface (a 30° edge). There were two rear discs: a metallic one of 30 mm Ø, protruding 12 mm

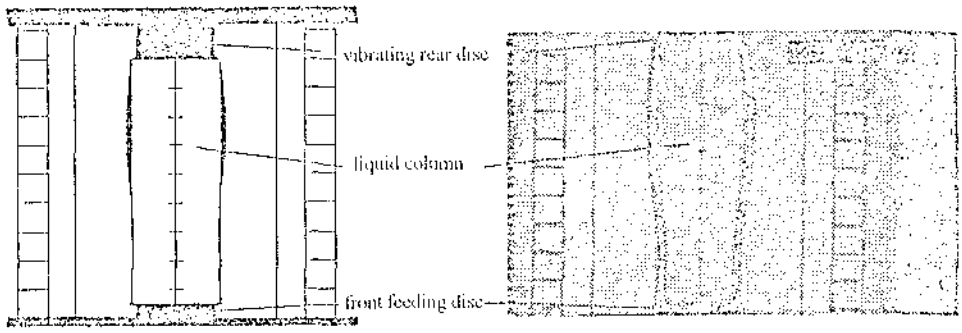

Fig. 1: Comparison between the ideal scene inside the AFPM test-chamber and the real one (in flight). The liquid column and the raster appear at different scales because of the conical perspective.

with 27 mm stem and a plastic one (PMMA) also of 30 mm. There were three front discs (all of them with a 10 mm hole for liquid feeding): a metallic 30 mm Ø, protruding 6 mm with 27 mm Ø, another metallic disc of 28 mm Ø, protruding 6 mm with 25 mm Ø and a plastic one (PMMA) of 30 mm Ø.

The working surface of the metallic discs was black anodised aluminum (AlMgSi 0,8) with a roughness of 0.3 µm CLA (ISO 468-1982), and the sides were antispread treated by baking a coating of 1.2 µm thickness of teflon (PTFE), plus brushing a coating of 3M-FC-723.

The interior of the AFPM test-chamber as seen by the videocamera is presented in Fig. 1 in two versions, the ideal scene imagined by the experimenter and the real one observed in flight. It may be argued that everything should have been known and accounted for, particularly for an experienced FPM investigator, but there are so many details and so little interaction (the flight equipment is inaccessible before flight, the engineering unit nearly the same, and the last details so decisive: working disc protrusion, raster design and fitting, etc.) that one cannot realistically be prepared for so many things. For instance, due to a late change in videocamera orientation, the image on SL-D-2 appears upside-down with respect to previous flights and to the crewman sight, so that now the front disc with the feeding hole is at the bottom (that is the disc that travels up and down), and the rear (oscillating) disc is at the top.

Diffuse background illumination by an array of 9x8 LEDs and a opaline glass diffuser was used to enhance the visualisation of the outer shape of the liquid column, although a meridian light sheet could be used if desired to visualise tracer motion inside. This AFPM illumination has gone a quantum step forward in optical quality (brightness and uniformity) compared to the crude performances of the old FPM in SL-1 and SL-D1.

Concerning the proposed and the executed experiment timeline there are also major changes because the matching of crew availability, audio and video links to ground, and so many needed resources in a stressed operational environment as Spacelab, has always proved to be an impossible fitting.

Two sequences of experiments (runs) were scheduled for STACO, the first one with equal discs as in SL-D1 and the second one either with unequal discs or with equal discs of a different material in case some kind of electrostatic effect were discovered. In flight, the first run (Run 1) started with one hour delay and the preparations (it was the first AFPM run) took some 30 minutes more than the 20 minutes allocated, so that in order not to run over the scheduled envelop the STACO experiment was stopped after only 30 % of the trials were performed (at the end of the vibration steps). As an example of contingency, many minutes were lost discussing through the voice loop and the photo recording abandoned because of a last-minute unnoticed change of photocamera model; an infancy problem similar to the unnoticed packaging of the FLIZ raster in SL-D1.

Unfortunately, due to the time shift, Run 1 was executed in the blind (not TV link) and the experimenters only gathered a short verbal report saying that the three frequency trials run nominally, and the middle one (at 0,41 Hz) seemed to be precisely the second eigenfrequency. Without further information before the second run was due to start, the investiga-

GMT ddd/hh:mm:ss	MET d/hh:mm:ss	Count s	L mm	V cm^3	Zoom*	Slant %	Notes
RUN-1							
118/11:13:47	1/20:23:47	55960	15	10.5	3.26	1.3	Start stretching. Run 1a (120 s)
118/11:14:00	1/20:24:00	55973	17.2	16.9	3.26	1.3	Good time origin
118/11:15:50	1/20:25:50	56083	85	59.5	3.26	1.3	End stretching
118/11:15:50	1/20:25:50	56083	85	59.5	3.26	1.3	End stretching: Run 1b (600 s)
118/11:25:10	1/20:35:10	56643	85	59.5	3.26	1.3	Start vibration
118/11:25:10	1/20.35:10	56643	85	59.5	3.26	1.3	Start vibration: Run 1c (300 s)
118/11:30:54	1/20.40:54	56987	85	59.5	3.26	1.3	End vibration
118/11:31:27	1/20:41:27	57020	85	59.5	3.26	1.3	Start vibration: Run 1d (100 s)
118/11:33:12	1/20:43:12	57125	85	59.5	3.26	1.3	End vibration
118/11:33:35	1/20:43:35	57148	85	59.5	3.26	1.3	Start vibration: Run 1e (150 s)
118/11:36:05	1/20:46.05	57298	85	59.5	3.26	1.3	End vibration
118/11:36:28	1/20:46:28	57321	85	59.5	3.26	1.3	Start vibration: Run 1f (100 s)
118/11:37:55	1/20:47:55	57408	85	59.5	3.26	1.3	End vibration
118/11:37:55	1/20:47:55	57408	85	59.5	3.26	1.3	End vibration: Run 1g (150 s)
118/11:40:35	1/20:50:35	57568	85	59.5	3.26	1.3	Start recover
RUN-2							
118/13:19.15	1/22:29:15	63488	15	10			Start stretching: Run 2a
118/13:20:55	1/22:30:55	63588	85	64			End stretching
118/13:20:55	1/22:30:55	63588	85	64	3.22	1.4	Start camera quiet: Run 2b (90 s)
118/13:22:18	1/22:32:18	63671	85	60	3.22	1.4	End camera quiet
118/13:22:32	1/22:32:32	63685	85	60	3.56	1.3	Start cam.quiet: Run 2c (200 s)
118/13:26:08	1/22:36:08	63901	85	60	3.56	1.3	End camera quiet
118/13:28:04	1/22:38:04	64017	85	60	3.17	2.3	Start camera quiet: Run 2d (13 s)
118/13:28:17	1/22:38:17	64030	85	60	3.17	2.3	End camera quiet
118/13:28:18	1/22:38:18	64031	85	60	3.17	1.7	Start cam.quiet: Run 2e (180 s)
118/13:31:15	1/22:41:15	64208	94	60	3.17	1.7	Breaking
RUN-3							
125/14:04.52	8/23:14:52	671025	15				Discs at 15 mm
125/14:07:07	8/23:17.07	671160	15	10	3.06	1.2	Bridge formed: Run 3a (300 S)
125/14:12:18	8/23.22:18	671471	15	10	3.06	1.2	Start stretching
125/14:12:18	8/23:22:18	671471	15	10	3.06	1.2	Start stretching: Run 3b (50 S)
125/14.13:07	8/23:23:07	671520	52	35	3.06	1.2	End stretching at 50 mm
125/14:13:07	8/23:23:07	671520	52	35	3.06	1.2	End stretching: Run 3c (20 S)
125/14:13:27	8/23:23:27	671540	52	35	3.06	1.2	Start stretching
125/14:13:27	8/23:23:27	671540	52	35	3.06	1.2	Start stretching: Run 3d (60 S)
125/14:14:27	8/23:24:27	671600	80	59	3.06	1.2	End stretching to 80 mm
125/14:14:27	8/23:24:27	671600	80	59	3.06	1.2	End stretching: Run 3e (30 S)
125/14.15:10	8/23:25:10	671643	80	59	3.06	1.2	Start stretching
125/14:15:10	8/23:25:10	671643	80	62	3.06	1.2	Start stretching: Run 3f (10 S)
125/14:15:25	8/23:25.25	671658	84	62	3.06	1.2	End stretching
125/14:15:25	8/23:25:25	671658	84	66	3.06	1.2	End stretching: Run 3g (180 s)
125/14:18:15	8/23:28:15	671828	84	66	3.06	1.2	Breaking

Table 1: SL-D-2-FPM-STACO timeline as flown.
Zoom figures mean number of horizontal pixels per mm in the raster plane.

tor chose to come back to the last executed step in the previous run and follow on with the same working discs.

The liquid column was restablished, what we mark as Run 2, although due to the time constraint, one air bubble of 8 mm in diameter was ingested in the working oil. Then the investigators on ground had for a first time a view of the liquid column (real-time TV), but noticed that the edges of the column were out of screen and instructed the crewman to zoom-out a little bit, what happened to be a time-wasting interaction since it was the output video-signal from the frame grabber and not the original signal that was clipped. Because experience had shown that breaking a liquid column by isorotation is more dangerous (to loose control of the liquid mass) than breaking by disc separation, the investigator asked the crewman to exchange the order of trials. Unfortunately, in spite that in SL-D1 there were five column breakages and the liquid always remained well-anchored and could be merged easily, in SL-D-2 this first breakage and all the rest happened to be catastrophic (waste of liquid control by overspreading to the back-side of the rear disc) and the experiment had to be terminated prematurely to allow sufficient time to clean-up before the next experiment.

The D-2 team managed to allocate an extra run for STACO, but problems with the AFPM power-up sequence prevented even to start. Fortunately the AFPM was recovered and the extra run for STACO (Run 3) was finally executed a week after. For still unknown reasons, the 84 mm long liquid column between unequal discs of 30 mm and 28 mm was trembling for more than three minutes without apparent stimuli until it broke, in an unrecoverable manner as before.

Data Analysis

Three sets of data were foreseen: the first and main one was the video recording (either real-time link or stored aboard), the second was the AFPM housekeeping data of disc position, volume injected, and values of applied stimuli, and the third one was a 35-mm photocamera 36-exposure film to be used only as high resolution samples.

It must be said from the beginning that the quality of the SL-D-2 video link was much better than expected from past experience on Spacelab and TEXUS, and also that the AFPM house-keeping data presentation in real-time was an achievement in comparison with the old status screen for SL-1 and SL-D1. Even the photocamera, that was prematurely abandoned for lack of confidence as explained above, did perform flawlessly and furnished the best available pictures of a large liquid column in space.

Problems with house-keeping data from the AFPM are minor: as said before, some of the tolerances enter into the working range (f.i. for low frequencies), some lagging has been discovered in the start of disc separation, and the fact that non-operating channels were full of noise instead of calm.

Problems with the video data, on the contrary, are important and plentiful, as can be grasp from the following list:

- Real images were seen only during the actual flight (plus one demo simulation of very little quality).
- The changes in video signal standard (NTSC to PAL) greatly impoverishes the quality of the video signal.
- Videotape recording (a VHS copy) has been used for all the analysis, the analogue video signal making difficult the repetition of time sequences.
- Conical perspective introduces scales and parallax deformations.
- Camera zoom and pan (and the associate rotation due to an eccentric pivoting) make video analysis too cumbersome.
- Misalignment through the optical axis (three intermediate mirrors) introduces a slant deformation.
- Frame grabber clipping was a big handicap during flight operations and for later analysis.
- Defocusing of the grid introduces large uncertainties.
- The smallness of the disc cutback introduces the largest uncertainty in the image analysis.

Fortunately, time and space references engraved on each videoframe have helped a lot in correlating sequences.

An account of the uncertainties related to image analysis follows. It is important to keep in mind that because of the conical perspective and the non-square pixel used, four different length scales can be used in an image: millimetres at the background raster (mm_ras), millimetres at the object plane or meridian cut of the liquid column (mm_obj), pixels along the horizontal direction of the frame grabber (px_hor) and pixels along the vertical direction of the frame grabber (px_ver).

The distance from the liquid column axis to the videocamera is taken as 800±5 mm (the uncertainty due to the several dioptrics interposed). The distance from the liquid column axis to the background raster is taken as 80±1 mm (uncertainty due to the dioptrics interposed). With those numbers (see Fig. 2) some apparent sizes are:

- The length of 85 mm_obj is seen as 85·(800+80)/800=93.5±0.6 mm_ras.
- The diameter of 30 mm_obj is seen as 30·(800+80)/800=33±0.2 mm_ras.
- The disc parallax at 50 mm off-axis gives a 50·30/800·(800+80)/800=2.0 mm_ras apparent size (minor axis of the ellipse).

The video-digitiser used (a Data Translation DT 2862 plug-in board) takes non-square pixels of a clipped video frame, resulting in a 1 px_hor/mm = 0.685±0.001 px_ver/mm ratio or a 1.460±0.002 px_ver/mm = 1 px_hor/mm ratio, according to a high precision test performed in-house.

Zooming changes the px-to-mm ratio and the origin for liquid shapes, as well as for panning, what, added to the in-the flight mode of video digitisation, renders these scenes (changing zoom or pan) useless for accurate analysis, so that the classification of useful scenes presented in Table 1 was based on that.

With the equipment used, only odd or even videolines can be scanned on the same frame due to synch problems, what have contributed the most to the uncertainty to accurately detect disc edges. The disc cutback of 0.9 mm only gives a 2 or 3 pixels trace (it should had been built to 5 mm, decreasing the diameter of the stem accordingly, at least locally).

When an image (as in Fig. 1) is digitised and analysed, the grey-levels at every pixel show profiles of the kind presented in Fig. 3, where the raster-print can be discerned. Looking in detail at such grey-level profiles one can find the following results.

The edge detection algorithm used defines the edge position as the location of the extreme of the first derivative (position of the peaks at the bottom of Fig. 3a), fitting the discrete values to a parabola, what assures a typical uncertainty of 0.1 pixels for the kind of profiles obtained in SL-D-2.

It is amazing to note that the levelling of the field of view, that was left to the crewman sight, appears to be always tilted clockwise, according to the figures of slant given in Table 1 (a 1.4% slant for Run 2b means that the corresponding horizontal reference line, 100 mm_ras to the right, is (1.4/100)*100=1.4 mm_ras below (3 px_ver) as can be appreciated f.i. at the bottom of Fig. 1b.

For the zoom corresponding to Run 2b, the 1 mm_ras reference line thickness gives 4.1±0.1 px_hor and 5.8±0.1 px_ver width, instead of the 3.22 px_hor and 3.22*1.46=4.7 px_ver ac-

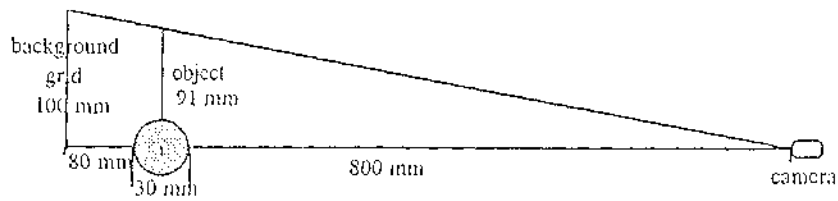

Fig 2: Optical scheme (without the optical bending and the mirrors) to appreciate the effect of parallax in the video image recording. A 30 mm in diameter liquid column is shown in profile.

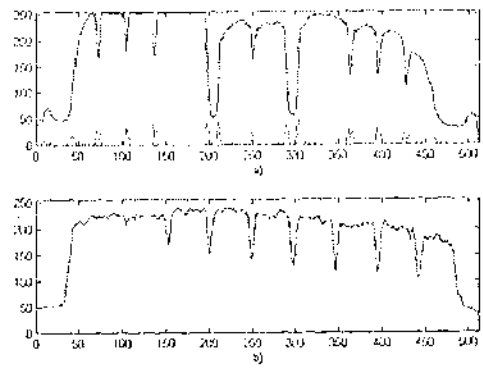

Fig. 3: a) Grey-levels of a mid-heights horizontal line of an image of Run 2b showing from left to right the three reference lines, the left border of the liquid column, the axial reference line, the right border and the other three reference lines. The absolute value of the first derivative is also plotted at the bottom. b) Grey-levels of a near-axial vertical line of the same image were the reference tick marks of the raster centre-line can be appreciated. White background should have a 256 grey-level. Black raster lines, because of defocusing, have mid grey-levels.

cording to Table 1, so the rest is due to defocusing. On the other hand, the 10 mm_ras line spacing of the square reference boxes gives 32.3±0.1 px_hor and 47.4±0.2 px_hor, practically equal to the 32.2 px_ver and 3.22·1.46=47.0 px_ver estimations with perfect focusing. By the way, the horizontal-to-vertical pixel size ratio obtained from the raster is (47.4±0.2)/(32.3±0.1)=1.47±0.01, in accordance to the calibration (1.46±0.005).

The 27 mm_obj width of the disc stem (that makes the disc protruding from the AFPM base-plate), gives 95.5±0.1 px_hor width, perfectly matching the 27·3.22·880/800=95.6±0.2 px_hor). Similarly, the 30 mm_obj width of a cylindrical liquid column (or at least near the discs), gives some 105.5±0.1 px_hor width, also matching the 30·3.22·880/800=106±0.2 px_hor).

The 0.9 mm_obj vertical projection of the cutback of the discs only allows for 0.9·3.22·1.46=4.2 px_ver, that is only two! odd pixels, meaning that the uncertainty in the column length as measured from the image is 0.5 px_ver or 0.1 mm_obj, whereas column radii (assuming a circular cross-section) is measured with an uncertainty of 0.1 px_hor (0.03 mm_obj). However, when only relative vertical position was needed, the (30-27)/2=1.5 mm_obj horizontal projection of the cutback of one disc could be tracked to an uncertainty of 0.2 px_ver. Using this trick, the amplitude peak-to-peak of the applied axial vibrations in Run 1 was measured to be 100.2 px_ver, corresponding to 10/(3.26·1.46) = 2.1±0.05 mm_obj, perfectly matching the 2.0±0.1 mm setting at the AFPM.

Considering now the behaviour of the liquid bridge, let us begin by the vibration trials in Run 1. Figure 4 presents successive ¼ period images for a full period of 0.25 s corresponding to the forcing frequency of 0.40 Hz in Run 1c. Note that f=0.40 Hz was the nominal frequency setting, but the AFPM data gives f =0.39±0.01 Hz, although the image analysis gives the value f =0.40±0.005 Hz from the FFT spectrum of either the disc motion or the main response of the liquid shape, presented in Fig. 5, where the time stages corresponding to the images in Fig. 4 have been marked. Similar pictures can be obtained for Run 1d, Run 1e and Run 1f, and the following points are found:

The centres of the liquid column slices at ¼, ½ and ¾ of its length (starting at the vibrating disc), oscillate with a period of 4.5±0.1 s (first lateral eigenfrequency) as seen from the video camera (it is not yet clear if this motion is a sinusoidal vibration in the meridian plane or just the projection of a uniform circular motion, as a skipping rope); their ordinate shift is due to the tilting of the image in the field of view. To discern between these two options, the motion of the big bubble in Run 2 and the difference in apparent optical position of the tic-marks behind the liquid dioptric have been tried, but without conclusive results.

The radii of the liquid column slices at ¼, ½ and ¾ of its length (starting at the vibrating disc), oscillate with a period of 2.5 s (the forcing frequency) and a long beating with a period of 14±0.5 s (the first eigenfrequency, as can be predicted by theory [6-8]). However, although the lateral oscillations were symmetric to the mid-plane between discs, the radial

oscillations are clearly asymmetric, with the radius at ¼ oscillating in phase with the disc, the radius at ½ in counterphase and with a larger amplitude (demonstrating that it is very near the second eigenfrequency), and the radius at ¾ oscillating in a bizarre fashion with sinusoidal hills but flat valleys and with the smallest amplitude, as can be expected from its far position from the source.

The main peak in the respective spectrums are f =0.40±0.005 Hz for Run 1c, f =0.41±0.01 Hz for Run 1d, f =0.42±0.005 Hz for Run 1e and f =0.42±0.01 Hz for Run 1f. Note that in order to have a given accuracy Δf around a given frequency f with a known sampling rate of f_s, the number of data points needed is $Np = f_s/\Delta f$ (for instance, to measure f=0.40±0.01 Hz, sampling at the video frequency of f_s =25 Hz, one needs a sequence of Np=25/0.01=2500 data points). Also, to have at least three points inside the spectral interval Δf to minimise the leakage effect (to better define the peak in the FFT), one has to transform three samples of Np, $Np+\Delta Np3$ and $Np+2\Delta Np3$, were $\Delta Np3$ is the number of data points in a third of a period, that is, $\Delta Np3 = f_s/(3 \cdot f)$; i.i. $\Delta Np3$ = 25/(3·0.4)=21 points.

It is very interesting also to analyse the decay of a perturbation. At the beginning of Run 1b, just after the sudden stop of the cylindrical injection, the liquid bridge oscillates in the first mode with a period of 14±0.5 s (the first eigenfrequency) and has a half-damping time of some 40±5 s (time to decrease the amplitude to one half). At the end of the oscillation runs, it can be seen that the first axial mode has also a half-damping time of some 40±5 s, but the second axial mode (the one purposely excited) has a half-damping time of just 7±0.5 s. These results may be used to check the validity of theoretical developments of viscous effects [7, 9 and 10].

The second run (Run 2) was the first seen on the ground control centre, and there was a 8 mm in diameter air bubble inside. For unknown reasons, the cylindrical filling was overdone in volume, with an AFPM reading of 64 cm^3 instead of the nominal 60 cm^3, but the crewman noticed it and removed the excess of liquid in two 2 cm^3 steps (Run 2b). The first axial eigenfrequency had a period of 12±0.5 s at this volume of 64 cm^3 (Run 2b) instead of

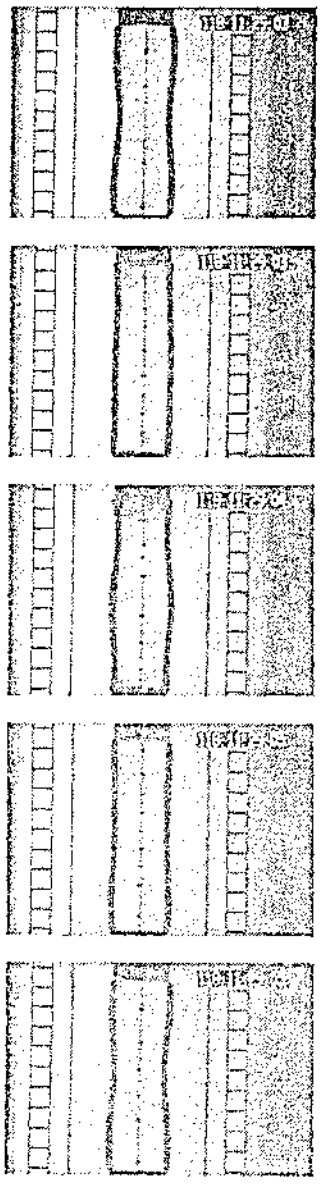

Fig 4: Video images sequenced at 0.6 s showing the full cycle at ¼ period intervals of an 85 mm long liquid column, 30 mm in diameter, vibrating during Run 1c. Forcing is by axial sinusoidal oscillation of the upper disc with 1 mm amplitude at 0.40 Hz. Distortion of the liquid column shape can be seen not only in the outer profile but in the refraction of the background raster marks.

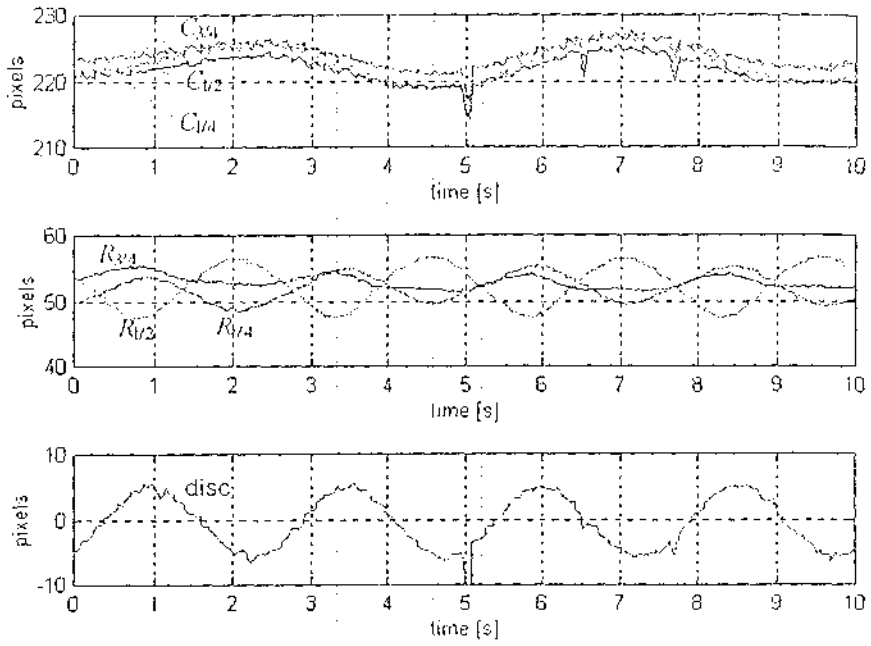

Fig 5: Evolution of three equispaced slices of the liquid column during Run 1c. The forcing is by up-and-down oscillations of the upper disc with an amplitude of 2 mm peak-to-peak (10 vertical pixels in the image) and a frequency of 0.40 Hz. The liquid column responds with radial oscillations in the second axial mode at the forcing frequency (the radius nearest to the forcing disc is $R_{1/4}$ and bulges when the disc pushes), and lateral oscillations in the first lateral eigenfrequency (all in horizontal pixels). The five dot-lines correspond to the pictures in Fig. 4.

the 13±0.5 s for the cylindrical volume at of 60 cm^3 (Run 2c). The accuracy in liquid volume metering, or the effect of the bubble, may explain the difference between the 13±0.5 s in Run 2c and the 14±0.5 s in Run 1 for apparently the same settings. Similarly, the first lateral eigenfrequency had a period of 4.8±0.2 s at the 64 cm^3 volume and 4.5±0.2 s at the 60 cm^3 of the cylindrical volume.

The extra run (Run 3) is plenty of unknowns and has yield little data, up to now, to check the extensive work on the behaviour of liquid columns between unequal discs [11-13]. It was performed one week after the other STACO runs, just after an extra run of the LICOR experiment. A small 15 mm long liquid bridge was left idle for more than 5 minutes due to drop-outs in the voice link. A rosary of steps in length and volume (L=15,52,79,80 and 84 mm and V=10,36,43,58,62 and 66 cm^3) was followed, instead of the direct step from L=15 mm to L=85 mm and V=10 cm^3 to V=58 cm^3 of the nominal procedure. A residual reading from the AFPM data of the frequency threshold (0.1 Hz) and the amplitude threshold (0.1 mm), just near the first axial eigenfrequency, throws no light.

During the very small period of Run 3c, with L=52 mm and V=36 cm^3 the liquid column oscillates axially with a period of 3±0.5 s. During the small period of Run 3e, with L=79 mm and V=58 cm^3 the liquid column oscillates laterally with a period of 4±0.5 s and a maximum amplitude of 4 px_hor peak-to-peak, and in the first axial mode with a very minute radial amplitude (tenths of a pixel) and a period of 10±1 s. During the long period of Run 3g with L=84 mm and V=66 cm^3 the

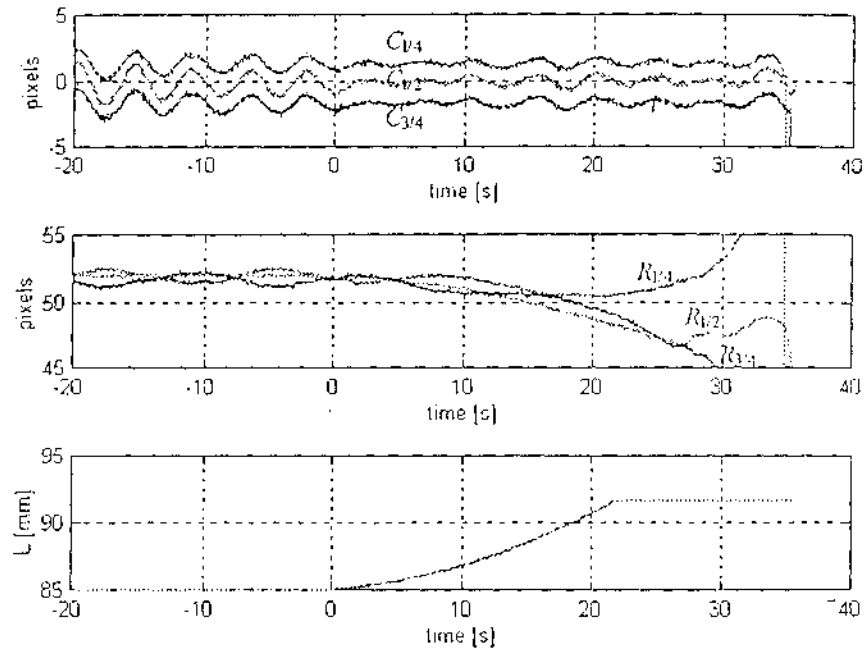

Fig. 6: Breaking evolution in Run 2e caused by disc separation at constant liquid volume. The initial liquid column shape was almost cylindrical, 85 mm long, 30 mm in diameter and 60 cm^3 in volume, and separation started at time 0, as seen in the position of the lower disc deduced from the video images (unfortunately the disc goes out of sight at 92 mm, before the 94 mm stop. Lateral oscillations of the center line (Cs) and radial evolution (Rs) are shown at three initially equispaced column sections (but the same video-lines are scanned during the stretching).

liquid column oscillates laterally with a period of 4.5±0.2 s and a maximum amplitude of 12 px_hor peak-to-peak, and in the first axial mode with a period of 12±0.5 s and a maximum amplitude of 4 px_hor peak-to-peak until at a certain stage and without previous notice the bulge of liquid, that had been all the time (oscillating) in the upper part, moved to the lower half and in the subsequent swing surpassed the stability limit and the column broke (see Fig. 7), unrecoverably as in the former cases.

With respect to the residual axial acceleration, or more precisely with the steady averaged deformation of the liquid outer shape, the extrapolation (accounting for only the difference in disc size) from the SL-D1 measurement of 70 μg [3], predicted for SL-D-2 a steady radial deformation from the cylindrical shape of 3 px_hor bulging in the feeding disc side ($R_{3/4}$) and of 3 px_hor necking in the rear disc side ($R_{1/4}$). The findings however do not support this extrapolation. Instead of this difference of $R_{3/4}$- $R_{1/4}$=6 pixels, STACO yields 0.6 pixels for Run 1b, 0.2 pixels for Run 2b and Run 2c, and 0.3 pixels for Run 2e. For Run 3, because of the difference in disc size, the correlation is much more involved and has not yet been worked out.

In any case, even before explaining the wide difference between the average deformation in Run 1 and Run 2, it can be concluded that the measured averaged deformation in SL-D-2 is one order of magnitude smaller than in SL-D1, so that the equivalent axial acceleration is of the order of 5±2 μg, in contrast to the 70±10 μg in SL-D1.

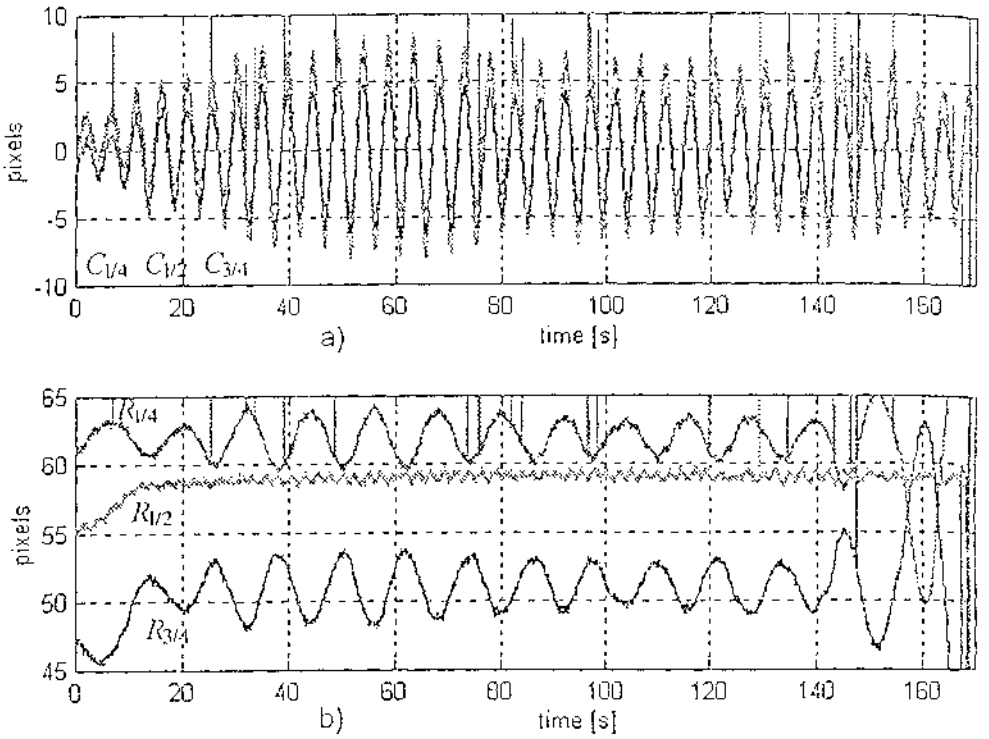

Fig. 7: Evolution during Run 3g. A liquid column 84 mm-long spanning between discs of 28 mm (bottom disc) and 30 mm in diameter (top disc), with 66 cm^3 of liquid, oscillating laterally (a) and axially (b), without known applied stimuli, for nearly 150 s until it unexpectedly breaks. Nomenclature is as in Figs. 5-6.

Results and Conclusions

The STACO experiment belongs to a series of microgravity experiments on the mechanical deformation of long liquid columns that, although performed over a 10-year period, only amount to a few several-minutes trials performed in a hurried and stressed operating environment.

The main achievement of STACO is the high accuracy reached in automatic image analysis, of the order of 30 μm in object size (0.1 pixels in the 512×512 image), what is a great improvement if compared to the manually digitised hard-prints in SL-D1-FPM-FLIZ.

The response of the 85 mm-long cylindrical liquid column to a forced axial vibration of one of the supporting discs is in very good agreement with the theory, and complements other measurements performed in the same flight (see LICOR report) with shorter columns.

Many unnoticed characteristics of the equipment, the optical set-up and the data acquisition system have been discovered that should be improved in future trials.

Some of the STACO objectives (isorotation trials and unequal disc vibration and rotation) had to be abandoned because of the unexpected over-spreading of the liquid to the back of the disc (in spite of the sharp cutback and the anti-spread coating), that consumed a lot of the allotted time. In SL-D1, on the

contrary, there were five breakings and mergings without liquid loss.

The more puzzling question left after the STACO trials is the lack of reproducibility of the steady averaged deformation measurement, perhaps because it is not a characteristic of the configuration and may be dependent on details of hardware (i.i. materials used, rounding of wetted corners, etc.) that escape to the control of the experimenter and are different in each campaign. As usual, more experiments are needed to elucidate the unexpected results of this one, but a clear progress in the overall experiment planning is evident.

Acknowledgement

The invaluable help of our student J.E. Moreno in programming the video frame grabber, the assistance of the ESTEC and SL-D-2 teams (particularly to the crewmembers H. Schlegel and U. Walter), and the financial support of the Spanish Grant from the CICYT ESP92-0001-CP, is acknowledged.

References

[1] Martinez, I., Liquid column stability. *Experiment J-ES-331, in Materials Science under Microgravity. ESA SP-222, pp. 31-36, 1985.*

[2] Martinez, I. & Meseguer, J., Floating liquid zones in microgravity, *in: Scientific Results of the German Spacelab Mission D1, Sahm, P.R., Jansen, R., Keller, M.H. (Eds.), DFVLR, Köln, FRG, pp. 105-112, 1987.*

[3] Martinez, I. & Sanz, A., Experiments with long liquid bridges under microgravity, *in Materials Science under Microgravity, ESA SP-295, pp. 413-419, 1990.*

[4] Martinez, I., Meseguer, J. & Perales, J.M., 1991, Stability of Long Liquid Columns, *in "ResearchProgram of the German Spacelab Mission D-2", Sahm, P.R., Keller, M.H., Schiewe, B. (Eds.), Wissenchaftliche Projektführung Spacelab Mission D-2, pp 221-222.*

[5] Bezdenejnykh, N.A., Meseguer, J. & Perales, J.M., 1992, Experimental Analysis of Stability Limits of Capillary Liquid Bridges, *Physics of Fluids A. Vol. 4, pp. 677-680.*

[6] Meseguer, J., Sanz, A. & Perales, J.M., 1990, Axisymmetric Long Liquid Bridges Stability and Resonances, *Appl. Microgravity Tech., Vol. 2, pp. 186-192.*

[7] Perales, J.M. & Meseguer, J., 1992, Theoretical and Experimental Study of the Vibration of Axisymmetric Viscous Liquid Bridges, *Physics of Fluids A. Vol. 4, pp. 1110-1130.*

[8] Nicolas, J.A., 1991, Frequency Response of Axisymmetric Liquid Bridges to an Oscillatory Microgravity Field, *Microgravity Science and Technology, Vol. 4, pp. 188-190.*

[9] Meseguer, J. & Perales, J.M., 1991, Viscosity Effects on the Dynamics of Long Axisymmetric Liquid Bridges, *Microgravity Science and Technology, Vol. 4, pp. 139-142.*

[10] Meseguer, J. & Perales, J.M., 1992, Non-steady Phenomena in the Vibration of Viscous Cylindrical Long Liquid Bridges, *Microgravity Science and Technology, Vol. 5, pp. 69-72.*

[11] Perales, J.M., Meseguer, J. & Martinez, I., 1991, Minimum Volume of Axisymmetric Liquid Bridges between Unequal Disks in an Axial Microgravity Field, *Journal of Crystal Growth, Vol. 110, pp. 855-861.*

[12] Martinez, I., Perales, J.M. and Gomez, M., 1992, Effects of Axial and Centrifugal Forces on the Stability of Liquid Bridges, *ESA SP-333, pp. 123-130.*

[13] Bezdenejnykh, N.A. & Meseguer, J., 1991, Stability Limits of Minimum Volume and Breaking of Axisymmetric Liquid Bridges between Unequal Disks, *Microgravity Science and Technology, Vol. 4, pp. 235-239.*